Individual aerosol particles from biomass burning in southern Africa: 1. Compositions and size distributions of carbonaceous particles

Mihály Pósfai,[1] Renáta Simonics,[1] Jia Li,[2] Peter V. Hobbs,[3] and Peter R. Buseck[2]

Received 13 March 2002; revised 30 May 2002; accepted 2 June 2002; published 8 March 2003.

[1] Individual aerosol particles in smoke plumes from biomass fires and in regional hazes in southern Africa were studied using analytical transmission electron microscopy (TEM), which allowed detailed characterization of carbonaceous particle types in smoke and determination of changes in particle properties and concentrations during smoke aging. Based on composition, morphology, and microstructure, three distinct types of carbonaceous particles were present in the smoke: organic particles with inorganic (K-salt) inclusions, ''tar ball'' particles, and soot. The relative number concentrations of organic particles were largest in young smoke, whereas tar balls were dominant in a slightly aged ($\sim$1 hour) smoke from a smoldering fire. Flaming fires emitted relatively more soot particles than smoldering fires, but soot was a minor constituent of all studied plumes. Further aging caused the accumulation of sulfate on organic and soot particles, as indicated by the large number of internally mixed organic/sulfate and soot/sulfate particles in the regional haze. Externally mixed ammonium sulfate particles dominated in the boundary layer hazes, whereas organic/sulfate particles were the most abundant type in the upper hazes. Apparently, elevated haze layers were more strongly affected by biomass smoke than those within the boundary layer. Based on size distributions and the observed patterns of internal mixing, we hypothesize that organic and soot particles are the cloud-nucleating constituents of biomass smoke aerosols. Sea-salt particles dominated in the samples taken in stratus clouds over the Atlantic Ocean, off the coast of Namibia, whereas a distinct haze layer above the clouds consisted of aged biomass smoke particles. *INDEX TERMS:* 0305 Atmospheric Composition and Structure: Aerosols and particles (0345, 4801); 0315 Atmospheric Composition and Structure: Biosphere/atmosphere interactions; 0345 Atmospheric Composition and Structure: Pollution—urban and regional (0305); 0365 Atmospheric Composition and Structure: Troposphere—composition and chemistry; *KEYWORDS:* biomass burning, carbonaceous aerosol, individual particles, TEM

Citation: Pósfai, M., R. Simonics, J. Li, P. V. Hobbs, and P. R. Buseck, Individual aerosol particles from biomass burning in southern Africa, 1, Compositions and size distributions of carbonaceous particles, *J. Geophys. Res.*, *108*(D13), 8483, doi:10.1029/2002JD002291, 2003.

1. Introduction

[2] Biomass burning has a large impact on the atmosphere both regionally and globally [*Crutzen and Andreae*, 1990; *Levine*, 1991; *Penner et al.*, 1992; *Hobbs et al.*, 1997]. Among other effects, the production of smoke aerosol influences the radiative properties of the atmosphere, changes cloud properties, and impacts the atmospheric budget of a range of elements and compounds. Apart from a few studies [*Cachier et al.*, 1991; *Gaudichet et al.*, 1995; *Echalar et al.*, 1998], little information exists on the composition and mixing of individual particles within smoke plumes, or on the aging of smoke particles [*Cachier et al.*, 1995; *Reid et al.*, 1998; *Okada et al.*, 2001]. The aim of the current study was to obtain data on the chemical and physical properties of individual particles from biomass smoke plumes in southern Africa, and from air masses in the region that were affected by the smoke.

[3] The Southern African Regional Science Initiative 2000 (SAFARI 2000) [*Sinha et al.*, 2003, Appendix A] provided an opportunity to study aerosol particles produced by savanna burning. We used analytical transmission electron microscopy (TEM), including energy-dispersive X-ray spectrometry (EDS) and electron energy-loss spectroscopy (EELS), to study aerosol particles from several smoke and haze samples and from a set of cloud samples.

[4] We examined smoke from both flaming and smoldering fires (although the distinction is often not straightforward since different stages of the burn can be present simultaneously in adjacent areas) in order to assess the

[1]Department of Earth and Environmental Sciences, University of Veszprém, Veszprém, Hungary.
[2]Departments of Chemistry/Biochemistry and Geological Sciences, Arizona State University, Tempe, Arizona, USA.
[3]Department of Atmospheric Sciences, University of Washington, Seattle, Washington, USA.

0148-0227/03/2002JD002291$09.00

Table 1. Samples Analyzed in This Study

UW Flight Number	Date (2000)	Location	Type of Sample	Time (UTC)	Sample Number	Stage Number	Light Scattering Coefficient (m^{-1})	Comments
1815	17 August	Kruger National Park, South Africa	Haze	0829–0925	15-H2	2	1.88×10^{-5}	In boundary layer, at 1.2 km
					15-H3	3		
			Smoke	1025–1034	15-SS2	2	1×10^{-4}	Young smoke of smoldering and flaming fire
					15-SS3	3		
			Smoke	1128–1131	15-SF2	2	2.3×10^{-3}	Young smoke of flaming fire
					15-SF3	3		
1816	18 August	Medikwe Game Reserve, South Africa/Botswana	Haze	0856–0914	16-H1	1	2×10^{-5}	Background haze, upwind of prescribed fire, at 1.8 km
					16-H2	2		
					16-H3	3		
			Smoke	1103–1110	16-S3	3		32 km downwind of prescribed fire
1825	31 August	West of Beira, Mozambique	Haze	0942–1015	25-H1	1	5.56×10^{-5}	In boundary layer, en route to Mozambique coast, at 2.7 km
					25-H2	2		
					25-H3	3		
			Smoke	1140–1147	25-SY2	2	4.2×10^{-4}	Young smoke of smoldering fire
					25-SY3	3		
			Smoke	1226–1240	25-SA2	2	1.7×10^{-4}	16 km downwind of the same smoldering fire
					25-SA3	3		
1826	1 September	Kaoma, Zambia	Haze	0629–0735	26-H3	3	$(2–5) \times 10^{-5}$	Upper haze layer at 3.6 km, en route to Zambia
			Smoke	0925–0933	26-S3	3		Young smoke
1837	13 September	Walvis Bay, off Namibian coast	Cloud	0905–1044	37-C2	2		Below, in, and above marine stratus clouds
					37-C3	3		
			Haze	1132–1212	37-H3	3		Main, upper haze layer, at 3.9 km

differences in the properties of individual particles from both types of emissions. Smoke samples immediately above biomass fires were studied from four research flights that sampled fire emissions in the Kruger National Park, South Africa; in the Medikwe Game Reserve, South Africa/Botswana; west of Beira, Mozambique; and near Kaoma, Zambia. Samples were also collected from smoke plumes 32 and 16 km downwind from the fire sources in the Medikwe Game Reserve and near Beira. Although these "aged" smoke particles were still fairly young ($\leq$ 1 hour old), significant changes occurred in them compared to the particles in the smoke just above the fires.

[5] Persistent, stratified haze layers that seriously degrade visibility are striking features during the dry season in southern Africa [*Jury*, 2000]. Samples collected from layers of this regional haze provided an opportunity to study the particle types that occur in the hazes, and how their compositions and sizes compare with particles in young smoke. We analyzed haze samples from the four flights listed above, and from a sample collected above the Atlantic Ocean, off Walvis Bay, Namibia. In addition, haze aerosol particles associated with marine stratus clouds were analyzed; a list of samples is given in Table 1.

[6] Biomass burning produces mainly carbonaceous particles [*Andreae et al.*, 1998]. Since both elemental and organic carbon (C) occur in biomass smoke, the broad group of carbonaceous particles can include different particle types that have highly variable atmospheric effects. Whereas elemental C is thought to only occur in soot (or black carbon, BC), organic compounds may occur in any smoke particles, including soot. Single-particle studies have been scarce on biomass smoke particles, and so little information is available on the individual-particle level [*Gaudichet et al.*, 1995; *Liu et al.*, 2000; *Okada et al.*, 2001; *Ikegami et al.*, 2001] or on carbonaceous aerosols in general [*Katrinak et al.*, 1992, 1993; *Sheridan*, 1989; *Okada et al.*, 1992; *Pósfai et al.*, 1999]. Since carbonaceous particles are the least accessible among the major types of tropospheric aerosol particles for single-particle electron-beam methods, the lack of data is understandable.

[7] The mass of BC ranges from 10% to 30% of the total aerosol in particulate emissions from savanna fires [*Liousse et al.*, 1995; *Andreae and Merlet*, 2001]. Apart from C, important quantities of potassium (K), sulfur (S), chlorine (Cl), and silicon (Si) are emitted from biomass burning. Although emission factors have been measured for several types of vegetation [*Andreae et al.*, 1998; *Turn et al.*, 1997; *Artaxo et al.*, 1998; *Sinha et al.*, 2003; *Hobbs et al.*, 2003], details of the distributions of these elements on individual particles is not known.

[8] Analytical TEM is a powerful tool for characterizing individual aerosol particles because it provides simultaneous morphological, compositional, and structural information. However, it has limitations. First, TEM methods are labor intensive and require the continuous presence of the operator; therefore, the number of analyzed particles is relatively small and statistics are poor. Second, in the vacuum of the TEM and under the electron beam some compounds may be vaporized. We performed experiments with volatile organic acids ($C_6H_{10}O_4$ and $C_7H_6O_4$) and found that such particles immediately sublimate when the electron beam hits them, even when a very low-intensity beam is used. Thus, only the more refractory organic substances will remain and be observable in the TEM samples. Nevertheless, we found that analytical TEM is still extremely useful for characterizing biomass smoke and haze particles and is a unique source

of information on particle coatings, agglomeration, and possible atmospheric reactions.

[9] The strategy used in this study was to identify major particle groups based on morphology, composition, and behavior in the electron beam. We term the three most important particle types in biomass smoke plumes (1) ''organic particles with inorganic inclusions,'' (2) ''tar balls'' (carbon-rich, spherical particles), and (3) ''soot.'' In the haze samples, the most abundant particles were ammonium sulfates, either externally or internally mixed with carbonaceous particles. Sea-salt particles were present in the samples collected near or over the ocean, and characteristic biogenic particles occurred in most haze samples. Compared with other particle types, mineral and industrial particles formed a negligible fraction of the samples listed in Table 1. This paper focuses on the properties of carbonaceous particles. Changes in the relative concentrations, compositions, and size distributions of the major carbonaceous particle types are discussed and interpreted according to sample type. In an accompanying paper [*Li et al.*, 2003b] the results from mostly inorganic aerosol constituents are described.

2. Experiment

[10] Aerosol sampling was performed from the University of Washington's (UW) Convair-580 research aircraft [*Sinha et al.*, 2003, Appendix A]. For ambient aerosol (and for aerosol particles in clouds), sampling was done by routing outside air continuously into the aircraft through a 5 cm diameter stainless steel tube that removed aerosol particles larger than $\sim$5 μm diameter. Smoke plumes were sampled using a different technique; since the aircraft generally did not reside in a plume for long enough to collect sufficient material for analysis, a sample of plume air was collected in a 2.5 m^3 Velostat grab-bag (Hobbs, submitted manuscript, 2003) [*Hobbs et al.*, 2003]. The grab-bag system had an aerosol 50% cutoff diameter of about 4 μm, as larger particles were lost in the inlet and on the walls of the grab bag.

[11] We used a three-stage impactor (model MPS-3, California Measurements, Inc.) with nominal cuts at 2 and 0.3 μm (first stage $d > 2$, second stage $2 > d > 0.3$, and third stage $d < 0.3$ μm); we studied mainly the second- and third-stage samples. In some sample sets, there were only minor differences in the size distributions and compositions between particles from the two lower stages; in such cases data from the two stages were combined. Particles were collected on copper TEM grids. For most samples, we used TEM grids that were covered with a lacey Formvar supporting film. The particles attach to this film, and many extend over the holes of the lace, which is excellent for EDS or EELS analyses because spectra can be obtained with little or no background signal. Low backgrounds are especially important in analyzing carbon and oxygen on a supporting film that also contains these elements. During the flight to Namibia (UW flight number 1837), we used TEM grids covered with continuous Formvar films. The samples were stored in grid boxes in a desiccator and part of the time in air until studied in the TEM.

[12] TEM was performed using mainly a Philips CM20 TEM operated at 200 kV accelerating voltage and equipped with an ultrathin-window Noran Voyager energy-dispersive X-ray detector. Electron energy-loss images were obtained using a 125 kV Hitachi 7100 TEM with an attached Gatan Imaging Filter that acts as both a spectrometer and an imaging device. Additionally, a 200 kV JEOL 2000FX microscope was used for imaging and EDS analyses. Images of the particles were obtained at magnifications ranging from 5000 to 500,000.

[13] The sizes of particles were measured on digitized electron micrographs by fitting ellipses to the particle outlines and taking the average of the short and long axes of the best fitting ellipse as the particle diameter. Particle number size distributions were derived for tar balls, sulfates, and organic particles. The shapes of soot particles are highly irregular and therefore the size distributions of soot were not determined. The upper limits of the resulting size distributions may be affected by the inhomogeneous distribution of particles on the grids: larger particles pile up in the center, where particle overlap makes size measurements impossible. Outward from the grid centers, the particles are more sparsely distributed, and this is the general specimen region from which our analyses and size measurements were obtained. We cannot be sure whether the particles in the selected specimen regions represent the original size distributions, and larger particles are probably systematically ignored because they are likely concentrated in the pileup regions of the specimens. However, in samples that were affected by marine air, several micrometer-sized sea-salt particles occur in the same grid regions as do submicrometer carbonaceous particles, which suggests that large particles were not excluded from the size distributions. The lower ends of the size distributions may have been affected by poor collection efficiency of <300 nm particles on the TEM grids (section 3.2).

[14] Quantitative data for elemental compositions are all from EDS analyses from the CM20 TEM. We analyzed standards to obtain sensitivity factors (''k-factors'') [*Cliff and Lorimer*, 1975; *Pósfai et al.*, 1995] for thin-film analyses of C, O, Na, Mg, Si, S, Cl, K, and Ca. Spectra were acquired for 60 s, with the diameter of the electron beam adjusted to include the entire particle. Low-energy X-rays emitted by light elements are absorbed to a high degree within the specimen. Therefore, the data for C and O can be regarded as semiquantitative, especially if considering that most particles cannot be analyzed without at least some contribution from the Formvar film (which also contains C and O). Decomposition of the particles in the vacuum or under the electron beam further complicates EDS analyses. Changes in the TEM are visible, and we used a low-intensity electron beam to avoid decomposition during spectrum acquisition. Tar balls and soot particles did not show any changes in the beam, whereas inorganic inclusions in the organic particles were beam sensitive but still possible to analyze without damaging them. Particles that contained ammonium sulfate invariably changed under the electron beam; analyses of such particles indicates the composition of the residue after the majority of the particle evaporated. In general, even where the EDS results may not accurately reflect original particle compositions, the analyses show characteristic changes between groups of particle types and from specimen to specimen, and are thus useful for distinguishing certain groups of particles and for studying the trends of changes. Where considering compositions, we present compositional triangles [*Buseck and Pósfai*, 1999] that are useful for

emphasizing changes in the relative concentrations of selected elements.

[15] We used electron energy-loss imaging to obtain compositional information about the particles at high spatial resolutions. To our knowledge, except for the study of *Pósfai and Molnár* [2000], this method has not been used in aerosol research and is just starting to be used in mineralogy [*Moore et al.*, 2001]. The compositional maps are made using electrons that lost a specific amount of their energy in inelastic interactions with the atoms in the specimen. We can select the energy range and thus produce element-specific images in which the brighter areas correspond to larger concentrations of the selected element. In addition to compositional maps, it is also possible to obtain a map of the relative thickness of the particle by using certain parts of the electron energy-loss spectrum [*Egerton*, 1986]. In these maps, the particle thickness is proportional to pixel brightness. The significance of such maps is that in the TEM we see two-dimensional projections of particles, and by measuring their third dimension we can determine their morphology and volume. In this study we use the energy-loss maps to demonstrate the inhomogeneous distribution of inorganic inclusions in organic particles. Selected area electron diffraction (SAED) patterns were obtained from a few crystalline particles to identify their crystal structures and indirectly their compositions.

3. Results and Discussion

[16] Almost every aerosol particle collected from the biomass smoke plumes was carbonaceous, that is, their major element was C. Most particles in the haze samples also contained C since even the ammonium sulfate particles were coated with carbonaceous films. The relative concentrations of other elements showed greater variability than C, so we used the element compositions (particularly the concentrations of K, S, Cl, and Si), the typical morphologies, and the behavior of particles in the electron beam to distinguish particle types. In the following we will describe the main particle groups, then discuss the changes in relative particle number concentrations and compositions in various types of samples.

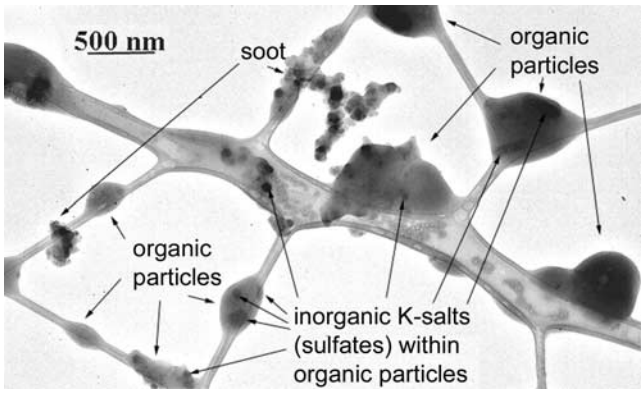

Figure 1. A typical portion of a sample of young smoke from a smoldering and flaming fire. Particles are attached to the lacey support film; most particles are carbonaceous (organic) with inorganic K-sulfate inclusions. As a result of diffraction contrast, the inclusions appear darker than the material of their host particles. (Kruger National Park, sample 15-SS3)

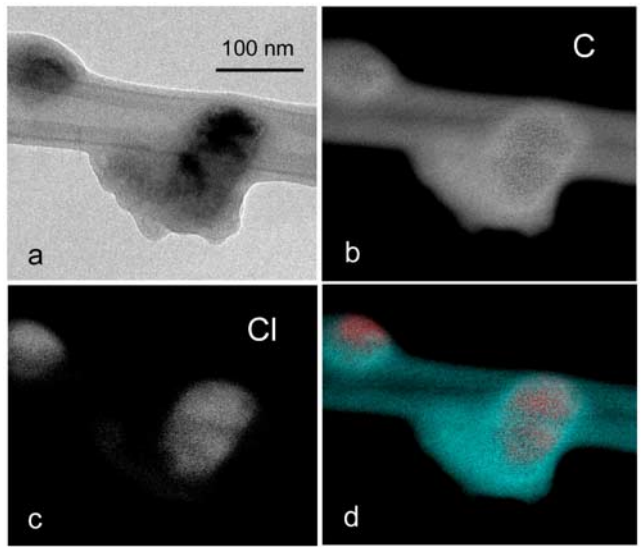

Figure 2. Electron energy-loss maps from two KCl-bearing organic particles that are attached to a thin ribbon of the Formvar support film. (a) Brightfield image, (b) C map, (c) Cl map, and (d) a composite image showing the distribution of C (blue) and Cl (red). In (a), the dark contrast within the inclusion results from diffraction by the crystalline substance. In (b) and (d), a fairly homogeneous distribution of C in the particles is shown, except for lower concentrations where the crystalline inclusions occur. Since the supporting Formvar substrate also contains C, there is intensity in the C map where the lacey film is present. The image in (c) indicates that Cl is only present in the inclusions. (West of Beira, Mozambique, sample 25-SY3)

3.1. Main Particle Types

3.1.1. Organic Particles With Inorganic Inclusions

[17] We termed the most abundant particle type "organic particles with inorganic inclusions," referring to the crystalline, visible inorganic constituents and the high C contents of particles that belong to this type. Organic particles with inorganic inclusions do not have distinct morphologies; they were probably hydrated on arrival onto the grid, and are usually spread along the "bars" of the lacey film and fill the corners of the holes (Figure 1). They typically contain crystalline K-salts, primarily either KCl or K_2SO_4, but the presence of KNO_3 was also inferred from compositional data [*Li et al.*, 2003b]. The bulk of the particles contain C and minor O and are stable in the electron beam. The compositions of the inorganic inclusions varied with age of the smoke, and probably the type of burnt vegetation; such variations are discussed below and in more detail in a companion paper [*Li et al.*, 2003b].

[18] The ratio of the mass of the inorganic inclusions to the mass of the whole particle is highly variable, but the majority of the particle mass is carbonaceous. Since the mole ratio of K/Cl is greater than 1 (and K/S > 2) for many of the particles in young smoke, additional K may be present within the carbonaceous material. The Cl content, however, is entirely contained within the inorganic inclusions, as indicated by energy-loss maps of the Cl distribu-

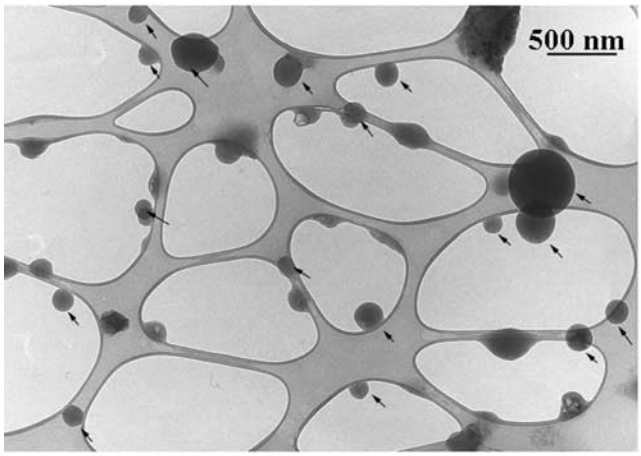

Figure 3. Spherical tar ball particles (arrowed) on a lacey supporting film. The sample is from aged smoke of a smoldering fire 16 km downwind from the fire. Particles that are not marked by arrows are organic particles with inorganic inclusions. (West of Beira, Mozambique, sample 25-SA3)

tion in such complex particles. Figure 2 shows two organic particles, each with a KCl inclusion. In the composite colored map blue corresponds to C and red to Cl. Such maps can be useful for detecting compositional inhomogeneities in a variety of particle types.

[19] Since our EDS and EELS analyses give elemental compositions, we have no direct evidence that C in these ''organic'' particles occurs in organic compounds. However, it is widely assumed that all of the elemental C in the tropospheric aerosol is within BC (soot) particles [*Jacobson*, 2001]. Because the organic particles with inorganic inclusions lack the typical morphological and microstructural features of soot, we assume they consist of organic substances. Nevertheless, organic particles were aggregated with soot, especially in aged smoke.

3.1.2. Tar Ball Particles

[20] Tar ball particles formed an important fraction of the total particle number concentration in some of the smoke plumes (Figure 3). Tar balls are spherical, amorphous, and stable in the electron beam and are typically not aggregated with other particle types. Neither inorganic inclusions as in ''organic particles'' nor turbostratic graphitic layers as in soot, occur in these particles. Since the methods we used do not permit the identification of organic compounds, the term ''tar ball'' only implies that the dominant element in these particles is C. They contain minor O, and trace amounts of K, S, Cl, and Si may also occur. Electron energy-loss maps show that the distribution of C and O in tar balls is homogeneous, and thickness profiles indicate that most are perfectly spherical (Figure 4). This characteristic shape likely indicates that the tar balls nucleated from the gas phase within the plumes.

[21] The distinction between organic and tar ball particles is somewhat arbitrary, since both the morphologies and compositions of the two groups overlap. Some particles assigned to the tar ball group on the basis of their lack of visible inclusions have slightly elongated shapes, and organic particles that contain inclusions may have spherical morphologies. Nevertheless, when the two types of particles are distinguished on the basis of their morphologies and the

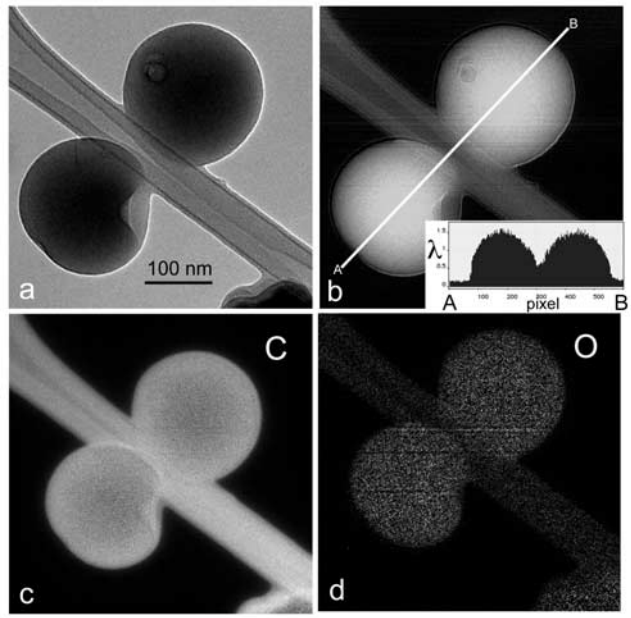

Figure 4. Electron energy-loss maps from two tar ball particles. (a) Brightfield image, (b) thickness map, (c) C map, and (d) O map. The inset in (b) shows a thickness profile from A to B. (On the vertical axis, λ stands for the mean free path; $\lambda = 1$ means the thickness through which the electrons take part in only one inelastic scattering event. λ is about 150 nm in such relatively light material [*Egerton*, 1986].) (West of Beira, Mozambique, sample 25-SA3)

presence or lack of visible inclusions, the resulting two groups show a distinct difference in composition (Figure 5): in general, the organic particles contain higher concentrations of elements other than C and O than the tar balls.

3.1.3. Soot Particles

[22] The third major carbonaceous particle type, soot, is clearly distinguishable from the tar balls and organic types because soot particles consist of chain-like aggregates of 20–50 nm spherules (Figure 1). Soot has a distinct microstructure [*Buseck et al.*, 1987]: the individual spherules are made of nearly concentric but wavy graphitic layers, wrap-

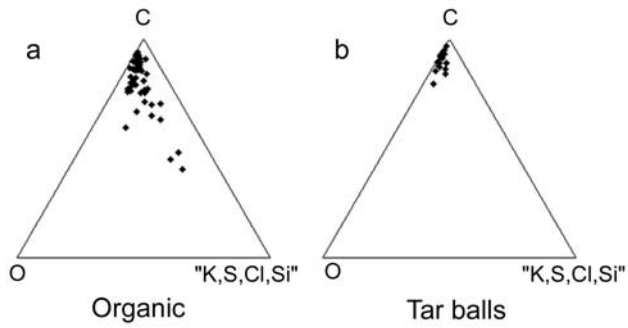

Figure 5. C, O, and ''other element'' (including K, Cl, Si, and S) contents of (a) organic and (b) tar ball particles. The triangles in (a) and (b) contain data from 53 and 24 particles, respectively, and all analyses were obtained from the young and aged smoke of a smoldering fire. (West of Beira, Mozambique, samples 25-SY2 and 25-SY3 versus 25-SA2 and 25-SA3)

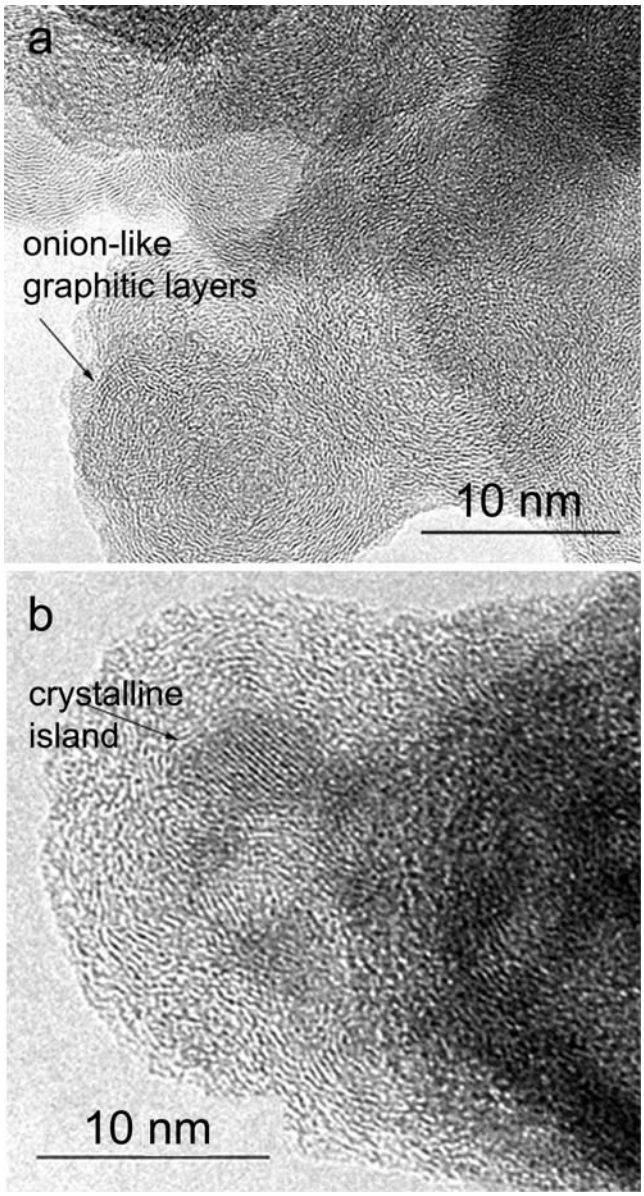

Figure 6. High-resolution TEM images showing the distinct microstructure of soot. (a) Individual spherules consist of turbostratic graphitic layers. (b) A few nanometer-sized graphite nucleus within a soot globule. (Kruger National Park, samples 15-SF3 and 15-SS2)

ped like the layers of an onion (Figure 6a). We have studied soot particles that originated from fossil fuel combustion [*Pósfai et al.*, 1999; *Pósfai and Molnár*, 2000]; compared with these particles, soot in the SAFARI samples had fairly ordered microstructures, and some particles even contained small islands of crystalline material (Figure 6b). The light extinction of soot particles increases with crystallinity [*Roessler et al.*, 1981]. Another typical feature of the SAFARI soot particles was that they contained minor Si; the electron energy-loss maps showed the Si to be evenly distributed within the particles.

3.1.4. Ammonium Sulfate Particles

[23] Ammonium sulfate is a major particle type in the haze samples, but it is almost absent from most of the smoke samples (with the exception of the sample taken 32 km downwind from the fire in the Medikwe Game Reserve, which may have been a mixed plume/haze sample). Ammonium sulfate particles were readily identified by their sensitivity to the electron beam: they decomposed under an intense beam and left behind a carbonaceous residue that originally formed a coating on the sulfate. Such internal mixtures of sulfates and organic compounds have been observed in a wide variety of continental and marine aerosols [*Pósfai et al.*, 1998, 1999; *Buseck and Pósfai*, 1999; *Pósfai and Molnár*, 2000; *Li et al.*, 2003a]. The relative thickness of the carbonaceous coating is variable, and its presence indicates that sulfates and organic compounds either condensed together or organic material formed on preexisting sulfate particles.

[24] A large fraction of the ammonium sulfate particles in several of the haze samples were internally mixed with either soot or organic particles, or both. In the samples from Namibia, submicrometer sea-salt particles were also mixed with ammonium sulfate.

3.1.5. Other Particle Types

[25] Sea-salt particles occurred in samples that were affected by marine air (e.g., those collected in Mozambique and Namibia). They can be identified by the constant ratios of Na, Mg, K, and Ca. The sea-salt particles typically had diameters of 1–3 μm, and their Cl and S contents were variable, depending on how aged they were. The compositions of sea-salt particles will be discussed further below, in relation to the Namibian cloud samples.

[26] Particles having interesting, flower-like morphologies occurred in several samples (Figure 7). They consisted mostly of C and O and also contained significant Si. They appear to be of biogenic origin, although their exact origin remains to be determined. They were most abundant in the haze sample collected over the Medikwe Game Reserve, but

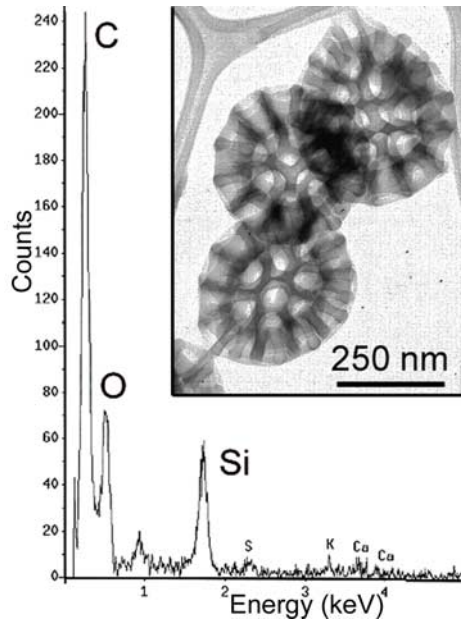

Figure 7. Unidentified, likely biological particles from background haze, and part of a typical EDS spectrum obtained from one such particle. (Medikwe Game Reserve, sample 16-H2)

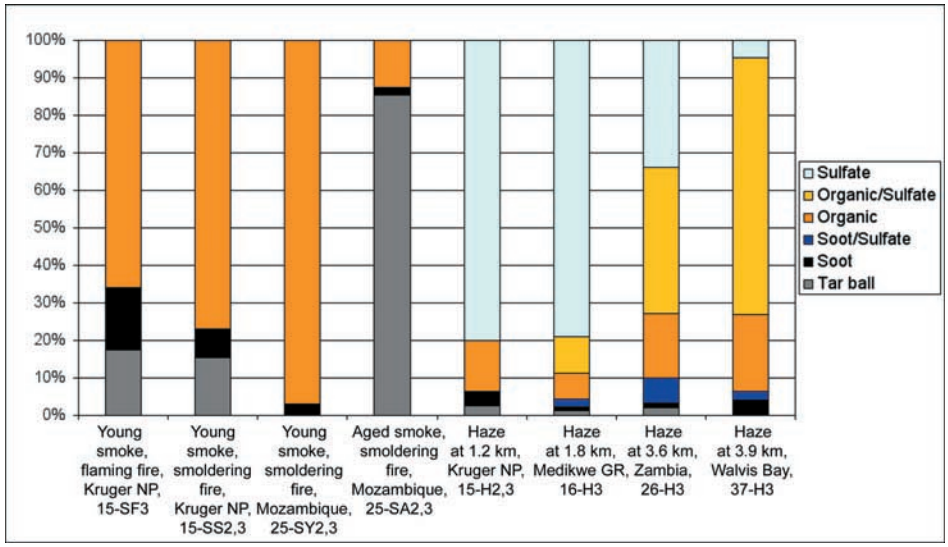

Figure 8. Relative number concentrations of the major particle types in various samples.

occurred in all haze samples, and also in some of the smoke plumes. Particles with similar morphologies and compositions were observed by *Ebert et al.* [2002] in continental air over Germany. Industrial pollutant particles, such as fly ash and metals, also occurred in some of the SAFARI samples; however, the relative number concentrations of these particles were so low that we will not discuss them further.

3.2. Changes of Particles With Type of Smoke and Aging

[27] In the following we discuss differences in particle-type concentrations and compositions in plumes from flaming and smoldering biomass fires, in young and aged smoke, and in the regional haze. Characteristic changes occurred in the relative number concentrations of the main particle types in the various samples (Figure 8).

3.2.1. Young Smoke From Flaming and Smoldering Fires

[28] Plumes from both mainly smoldering and mainly flaming fires (Kruger National Park, UW flight 1815, Table 1) allowed us to compare the individual particles emitted by these two types of fires. We studied second- and third-stage samples from the plume of the primarily smoldering fire (samples 15-SS2 and 15-SS3 in Table 1). Since relative particle concentrations were almost identical for these two stages, the observed particle numbers are combined in Figure 8. From the young smoke of the hotter, flaming fire, we studied a third-stage specimen (15-SF3). Organic particles dominated in the smoke from both fires, and a smaller number of tar ball and soot particles were also present. The relative number concentration of soot was about twice as large (16.5%) in the plume from the flaming fire than in the smoke from the smoldering fire (7.5%). Although this difference is small, it is consistent with several reports that flaming, higher-temperature fires emit a more absorbing, BC-rich smoke than smoldering fires [*Cachier et al.*, 1995; *Andreae et al.*, 1998; *Li et al.*, 2003b]. Tar balls were almost entirely absent from the fresh smoke of another smoldering fire (from Mozambique, UW flight 1825, samples 25-SY2 and 25-SY3 in Table 1), and the plume was also poor in soot particles (Figure 8). Soot and organic particles were typically not aggregated in young smoke.

[29] Size distributions of organic particles from the plumes of flaming and smoldering fires in Kruger National Park (Figures 9a and 9b), and a smoldering fire in Mozambique (Figure 9d), show a slight difference in that the flaming fire produced particles with a narrow size distribution and a single peak at about 200 nm (Figure 9b), whereas the organic particles from the smoldering fires had broader distributions and extended to larger sizes (Figures 9a and 9d). There is an uncertainty, however, with the size distributions of organic particles. These particles seem to have been hydrated and may have spread on the grid during drying. Thus, their sizes (as measured in the two-dimensional projections on TEM images) may not represent their original diameters. In contrast, tar ball particles from the same flaming fire in Kruger National Park (Figure 9c) have a unimodal size distribution similar to that of organic particles from the flaming fire, but the maximum concentration occurs at a smaller diameter, between 100 and 150 nm.

[30] To test the reliability of the TEM-derived size distributions (Figures 9a–9i), we compared two of these size distributions with those obtained from a PMS PCASP particle counter mounted on a wing of the Convair-580 aircraft [*Hobbs et al.*, 2003]. For the haze samples from Kaoma and Walvis Bay (UW flights 1826 and 1837, respectively), size data were combined for all types of particles on selected areas of the TEM grids. As mentioned in section 2, owing to the inhomogeneous distribution of particles on the grid, it is not possible to obtain absolute particle concentrations from the TEM data. However, the general shape of these distributions can be compared with those of the ambient (PCASP-derived) size distributions within the 100–1000 nm range (Figures 9j and 9k). The shapes of the two curves are in reasonable agreement for particles larger than about 300 nm, but smaller particles are underrepresented on the TEM grids. The reason for the absence of the majority of <300 nm particles could be either their high volatility (and thus their preferential removal in the vacuum of the TEM) or, more likely, a poor collection efficiency of small particles on the TEM grids.

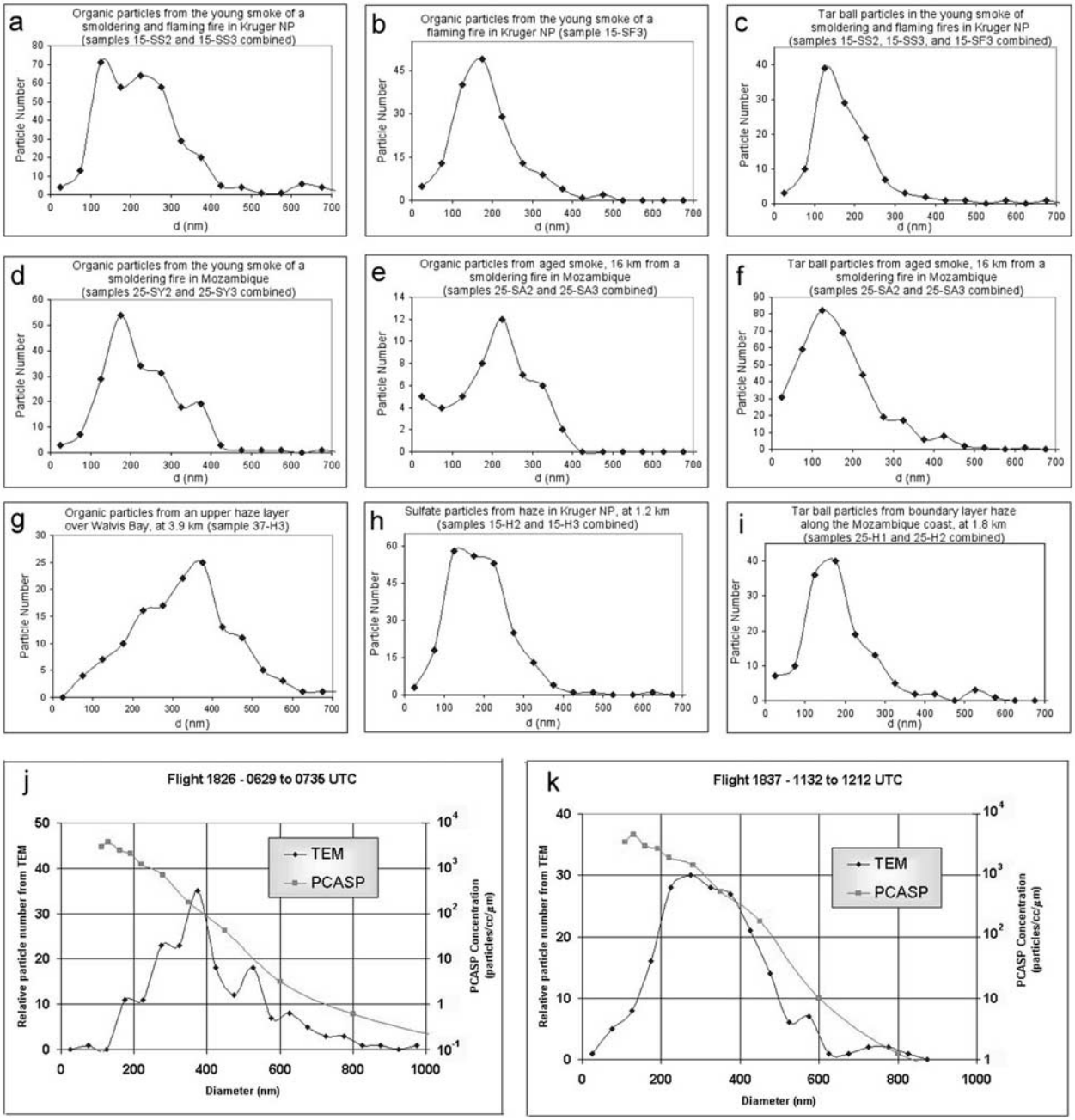

Figure 9. (a)–(i) Size distributions of organic, tar ball, and sulfate particles from selected samples, as indicated on each diagram. The sizes of particles were measured on digitized electron micrographs (see text for details). (j) and (k) Comparison of particle sizes as measured on TEM grids (''TEM'') with ambient size distributions obtained using an optical particle counter (''PCASP'').

[31] The compositions of particles formed in emissions by different fires are primarily a function of the fuel composition [*Turn et al.*, 1997; *Andreae et al.*, 1998]. However, the nature of the combustion also plays a role in determining particle compositions [*Cachier et al.*, 1995]. For example, the inorganic inclusions in organic particles from the young smoke of the flaming fire in the Kruger National Park consisted almost exclusively of KCl (Figure 10, first row, 15-SF3), whereas similar particles in the smoke of a smoldering fire from the same area contained mainly K_2SO_4 (samples 15-SS2 and 15-SS3, not shown in the figure). On the other hand, compositions of particles in the young smoke of the smoldering fire in Mozambique (Figure 10, samples 25-SY2 and 25-SY3) were similar to those emitted by the flaming fire. The second row in Figure 10 shows element ratios of particles from young smoke from burning of the Miombo vegetation type (Zambia; sample 26-S3); organic particles in this sample contained almost no Cl, and their S contents were also low. In general, we find that the Cl contents of particles in young smoke can be high, and the Cl/S ratio may be a function of both fuel composition and type of fire. Variations in the inorganic constituents of smoke

particles are discussed in more detail in a companion paper [*Li et al.*, 2003b].

3.2.2. Aging of Smoke

[32] Rapid changes occur in the relative concentrations of particle types with aging of the smoke, as illustrated in a set of samples from the smoke of a smoldering fire in Mozambique (UW flight 1825, Table 1). Tar ball particles were absent in the plume directly above the fire, but they were the dominant particle type just 16 km downwind (Figure 8, samples 25-SY2 and 25-SY3 versus 25-SA2 and 25-SA3). Considering the prevailing wind speed at 6.7 m s^{-1}, a distance of 16 km translates into a smoke age of about 40 min. It is likely that condensation from the gas phase produced the tar balls, since their spherical shapes indicate a gas-to-particle type nucleation mechanism.

[33] The size distribution of tar balls from the aged smoke of the Mozambique fire (Figure 9f) indicates practically no particle growth relative to the particles in the young smoke of other fires (in the Kruger National Park, UW flight 1815, Figure 9c), and the peak in the distribution at 100–150 nm is at the same diameter. Slight growth can be observed in the size distribution of organic particles from the aged smoke of the Mozambique fire (Figure 9e) relative to fresh smoke from the same fire (Figure 9d), although so few organic particles were measured in this sample that the statistics for Figure 9e are poor.

[34] Compositions are shown for particles in two aged smoke samples, one from the Medikwe Game Reserve and another from Mozambique (Figure 10). The Medikwe sample contains particles of various ages because it was collected while flying from 32 km downwind toward the fire. The aged smoke particles contain higher concentrations of C and S and relatively less K and Cl than those from young smoke. In the case of the Mozambique sample, this compositional change reflects the aging of the entire smoke instead of individual particles, since in the aged smoke mostly tar balls were analyzed, whereas in the young smoke the compositional data are mainly from organic particles. Data for the Medikwe sample include analyses of organic, soot, and tar ball particles.

3.2.3. Particles in the Southern African Regional Hazes

[35] A continental anticyclone typically dominates over the southern part of Africa from August to October, creating stable inversion layers that trap pyrogenic emissions above the subcontinent [*Jury*, 2000] (H. Annegarn et al., "The River of Smoke": Characteristics of the Southern African springtime biomass burning haze, submitted to *Journal of Geophysical Research*, 2003). Aged products of biomass burning accumulate in haze layers that can extend over thousands of kilometers. Specimens were collected from haze layers at various altitudes during the SAFARI 2000 experiment; we distinguish the boundary layer haze (up to about 3 km altitude in daytime, lower haze) from elevated haze layers (upper haze). Ammonium sulfate particles are abundant in relative number concentrations and are both externally and internally mixed with the organic and soot particle products of biomass burning (Figure 8). A clear difference exists between samples in the lower hazes (Kruger Park and Medikwe) and the upper hazes (Zambia and Namibia). In the lower hazes only about 20% of the particles were directly affected by biomass burning, whereas 67% and 95% of all particles in the two samples from the upper haze contained a smoke component (e.g., organic, tar ball, or soot particles) (Figure 8). A likely explanation for this difference is that smoke particles were lofted to higher elevations by the heat of the fires, and then were dispersed fairly evenly above the boundary layer.

[36] The presence of a large number of externally mixed sulfate particles in the lower haze layers indicates that their nucleation was not facilitated by heterogeneous processes on biomass smoke particles. Most sulfate particles in these samples presumably result from processes other than biomass burning. Although S is emitted by biomass fires [*Andreae et al.*, 1998; *Andreae and Merlet*, 2001; *Sinha et al.*, 2003], industrial and biogenic sources of sulfate precursors can also be significant.

[37] The most abundant particles in samples from the upper haze layer belong to the mixed organic/sulfate type, and the concentrations of soot/sulfate mixed particles are also high (Figure 8). Mixtures of all three types occur as well; we place these either in the organic/sulfate or soot/sulfate group, depending on their main constituent. The volatile ammonium sulfate in the mixed sulfate/smoke particles is clearly distinguishable in the TEM from the more refractory carbonaceous constituents that apparently originated from biomass smoke. Both coagulation and heterogeneous nucleation of sulfate on smoke particles could have led to the formation of these internally mixed particles. A size distribution obtained from organic particles in the upper haze off the coast of Namibia (Figure 9g) clearly indicates the larger sizes and presumed growth of these particles relative to those in young and slightly aged smoke.

[38] Tar balls formed a minor group (0–3% of the total particle number) in every haze sample (Figure 8), and they were not aggregated with other particle types. The size distribution of tar balls in the haze from Mozambique (Figure 9i) is practically the same as their distributions in the young and aged smoke (Figures 9c and 9f, respectively), indicating that these particles were likely an inert, hydrophobic component of the aerosol. Externally mixed sulfate particles in haze over Kruger Park have a size distribution (Figure 9h) that is similar to those of the tar balls, indicating that similar processes (gas-to-particle conversion through homogeneous nucleation) likely formed both types of particles, even though the origins of their precursor gases may have differed.

[39] The number of analyzed samples is too small to determine whether the aged smoke sample from Mozambique was unique or whether the high concentration of tar balls is a general property of biomass smoke plumes after they reach a certain age. Organic vapors can condense from the gas phase, but some organic substances are depleted through chemical transformations during aging of smoke [*Reid et al.*, 1998; *Hobbs et al.*, 2003; *Yokelson et al.*, 2003; *Gao et al.*, 2003]. Conversion of organic compounds can even result in an increase of BC/C_{total} ratios downwind of the fire [*Liousse et al.*, 1995]. Although we do not know which compounds occur in the tar balls, we consider it possible that the appearance of tar balls in aged smoke is related to the chemical changes observed in bulk aerosol.

[40] The compositions of the haze particles that were sufficiently stable to be analyzed using EDS (i.e., those that had a significant smoke particle component) indicate that further aging of biomass smoke results in the total loss of Cl and the acquisition of excess S (Figure 10). In this respect,

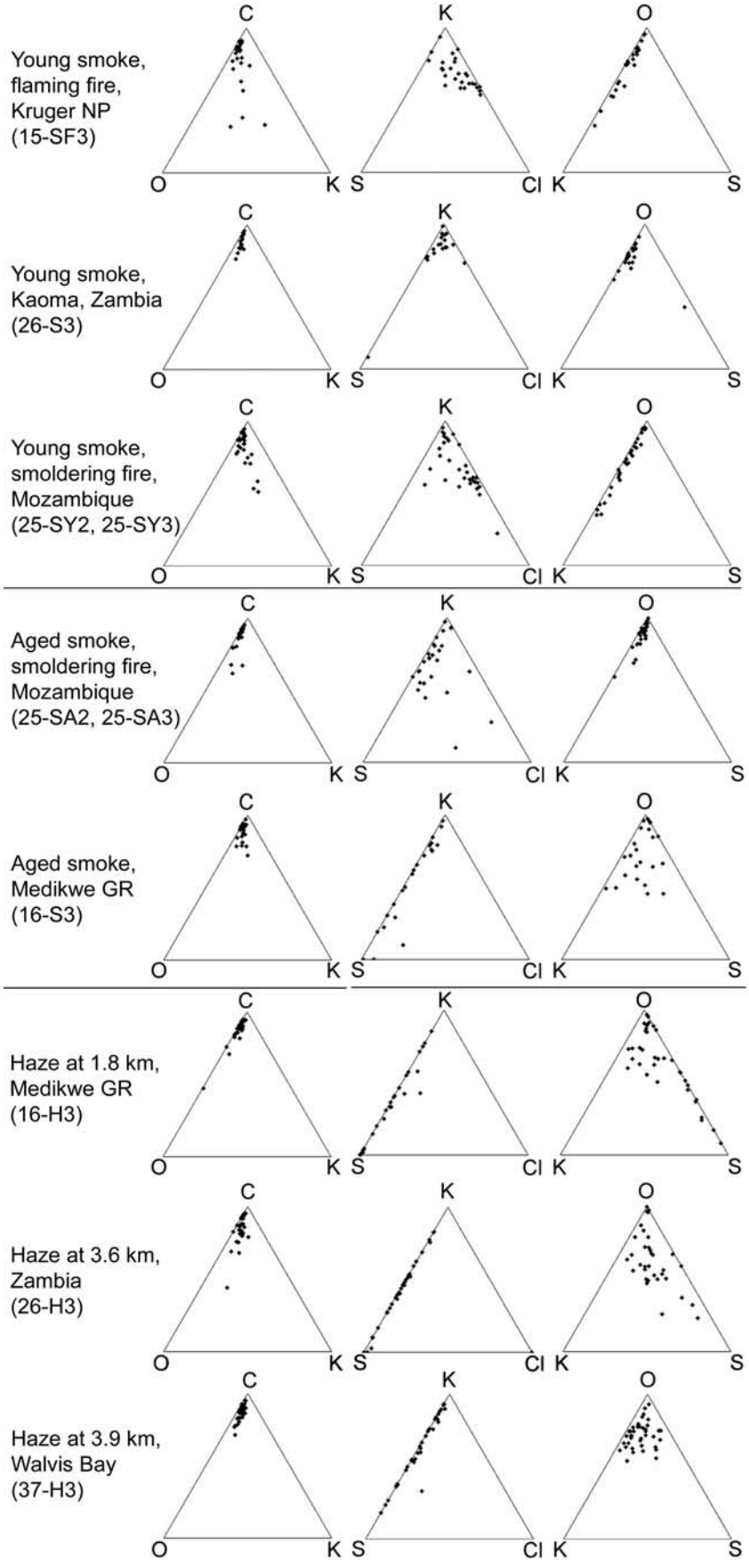
Young smoke, flaming fire, Kruger NP (15-SF3)
Young smoke, Kaoma, Zambia (26-S3)
Young smoke, smoldering fire, Mozambique (25-SY2, 25-SY3)
Aged smoke, smoldering fire, Mozambique (25-SA2, 25-SA3)
Aged smoke, Medikwe GR (16-S3)
Haze at 1.8 km, Medikwe GR (16-H3)
Haze at 3.6 km, Zambia (26-H3)
Haze at 3.9 km, Walvis Bay (37-H3)
C
K
O
S
Cl

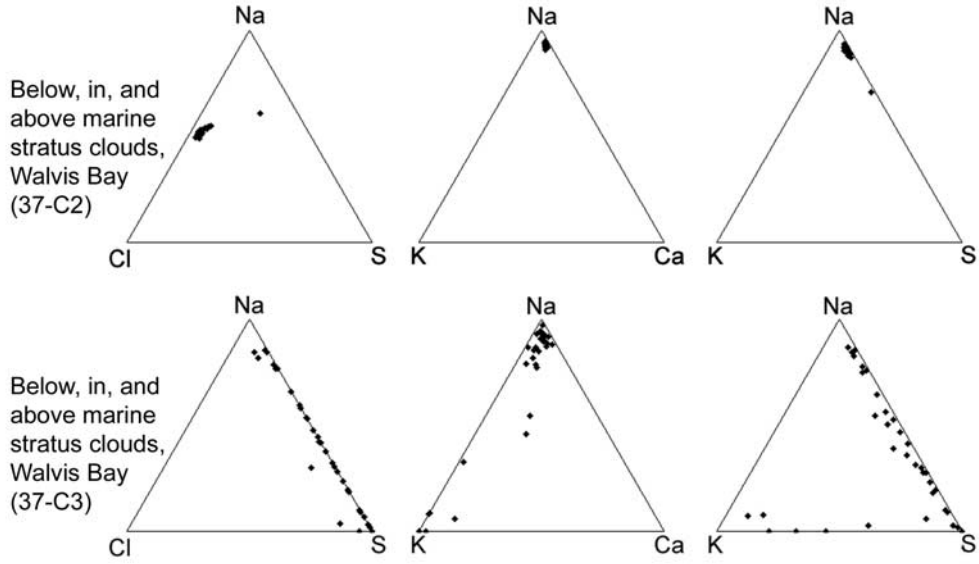

Figure 11. Relative concentrations of selected elements in a cloud sample, as determined by EDS analyses. The first row of triangles contains data from particles on the second stage of the impactor ($0.3 < d < 2$ μm), whereas the lower row contains data from the third stage ($d < 0.3$ μm).

we see no difference between the lower and upper haze layers: the smoke particles were aged and associated with S in both cases. It is also apparent that the aged smoke particles in the haze samples have more uniform compositions than those in young and slightly aged smoke. The uniformity of C/K ratios is most pronounced in the sample that was obtained from the upper haze layer above the Atlantic Ocean off Walvis Bay, Namibia. The wide range of K/S ratios in all three haze samples is attributable to the presence of variable amounts of excess sulfate on the smoke particles.

[41] Since ammonium sulfate particles sublimate under the electron beam, they cannot be represented in the compositional triangles. Even though the sulfate residue contributes to the measured S content of mixed organic/sulfate and soot/sulfate particles, it is not possible to distinguish smoke particles on the basis of their ''volatile sulfate'' contents in Figure 10. However, a marked difference is visible in the electron microscope between particles from the upper and lower haze layers: the smoke particles in the lower haze layer may or may not have a small volatile sulfate component, but most organic and soot particles in the upper haze samples were clearly aggregated with ammonium sulfate.

3.2.4. Aerosol Particles Associated With Marine Stratus Clouds Over the Atlantic Ocean

[42] During UW flight 1837 to Namibia, two distinct types of samples were collected, one from the upper haze layer at an altitude of 3.9 km (as discussed above), and another while the aircraft was flying below, in, and above stratus clouds that were capping the boundary layer. We studied second- and third-stage specimens from the cloud samples, and found a profound difference between the compositions of particles on the two stages.

[43] Particles on the second stage were all fresh sea-salt particles, with compositions reflecting the molar ratios of dissolved ions in seawater (Figure 11). Except for a single particle that had a high S content, all of the analyzed particles lie in one tight group in the compositional triangles, showing no signs of reactions in the atmosphere. By contrast, most particles on the third stage were fully aged sea salt; their seawater origin is indicated by their high Na contents and the fact that in the Na-K-Ca diagram many particles plot in one group near the apex of the triangle (Figure 11). However, Cl is entirely lost from these particles, and they contain excess S. It seems that smaller particles preferentially converted to sulfate, while supermicrometer sea-salt particles remained largely unreacted. In addition to aged sea salt, particles from biomass smoke also occurred in the third-stage specimen, as indicated by the high K contents of some particles. The likely origins of these particles is best seen from the Na-K-S diagram; data points along the Na-S line represent sea-salt particles with various amounts of additional non-sea-salt sulfate, whereas particles from biomass smoke (organic particles and soot) plot along the K-S line. Since there are no data points in the central region of the triangle, the sea-salt and smoke particles are mostly externally mixed.

3.3. Particle Properties and Possible Atmospheric Effects

[44] The three main carbonaceous particle types likely have different effects on the atmosphere. Tar balls are

Figure 10. (opposite) Relative concentrations of selected elements in particles from three young smoke samples, two slightly aged smoke samples, and three haze samples, as determined by EDS analyses. Ammonium sulfate particles are the major particle type in the haze samples (Figure 8). However, because of the high volatility of ammonium sulfate, only few of these particles were analyzed. Thus, the data in the compositional triangles for the haze samples represent mainly soot, organic, and organic/sulfate mixed particles. Triangles for the young and slightly aged smoke samples include data from organic, tar ball, and soot particles in approximately the same proportions, as indicated in Figure 8 for each sample.

typically not aggregated with other particle types; they show no signs of growth and seem to be typical constituents of smoke that has reached a certain age (Figure 3). These characteristics suggest that tar balls are not effective as cloud condensation nuclei (CCN). Tar balls were also a dominant aerosol particle type during the winter in the polluted continental aerosol above Hungary [*Pósfai and Molnár*, 2000] and in a haze layer over the Indian Ocean (Pósfai et al., unpublished results). Related meteorological and other aerosol chemical data suggest that in both cases the likely source of tar balls was biofuel combustion [*Pósfai and Molnár*, 2000; *Reiner et al.*, 2001]. We plan additional studies of these particles to explain the formation of tar balls in the SAFARI 2000 biomass smoke plumes and their virtual absence in the haze samples.

[45] Organic particles with inorganic inclusions were the dominant type in biomass smoke and in the regional hazes that were strongly affected by biomass smoke. The irregular morphologies of these particles suggest that they were hydrated on collection. At least part of their organic material may be water soluble. It is known that many water-soluble organic compounds occur in biomass smoke [*Crutzen and Andreae*, 1990; *Gao et al.*, 2003], and neither tar balls, nor soot seem likely candidates for containing significant amounts of such materials. Even if the carbonaceous part of organic particles were water insoluble, the inorganic K-salt inclusions should make the mixed particle hydrophilic. Thus, organic particles with inorganic inclusions are likely responsible for the high cloud-nucleating potential of biomass smoke particles [*Hobbs and Radke*, 1969]. Indirect conclusions can be drawn regarding the optical properties of organic particles: since organic particles dominate in biomass smoke plumes, and the net direct radiative forcing by biomass smoke is negative [*Hobbs et al.*, 1997], we assume that organic particles are not significantly absorbing in the visible range of the spectrum.

[46] Soot particles become progressively more aggregated with organic and sulfate particles during the aging of smoke. A wide variety of soot sizes is apparent in our samples, ranging from a few attached spherules that are smaller than 100 nm to micrometer-sized branching aggregates. The larger aggregates did not seem to occur in the haze layers, which could be a result of their formation conditions. Studies of diesel emissions [*Roessler et al.*, 1981] show that the air/fuel ratio affects the degree of agglomeration and volatile contents of soot particles. Those produced at low air/fuel ratios are highly agglomerated and consist primarily of elemental C, whereas particles are less agglomerated and contain considerable volatile organic material at high air/fuel ratios. We assume that air/fuel ratios can be highly variable for biomass combustion, resulting in the production of all types of soot particles. If indeed the smaller agglomerates contain more volatile organic material, they should be more likely to form internal mixtures with other aerosol species and to occur in internally mixed haze particles.

[47] Several studies show that internal mixing of soot with nonabsorbing species such as sulfate enhances the absorption efficiency of soot [*Haywood and Shine*, 1995; *Fuller et al.*, 1999] because the host particle acts as a lens that focuses more sunlight onto the absorbing core. According to *Jacobson* [2001], the primarily internal mixing state of soot in the global atmosphere results in a higher direct positive forcing than previously thought, making BC the second most important component of global warming after CO_2. In the optically thick haze layers encountered in SAFARI 2000, the majority of the soot particles were associated with either sulfates or organic particles (Figure 8), and thus their absorption efficiency presumably is significantly increased relative to that in young smoke.

[48] Organic and soot particles seem to be persistent aerosol types that survive smoke aging and transport on a regional scale. Biomass smoke particles (as identified by their K contents) can travel over long distances [*Andreae*, 1983], and soot and soot/sulfate aggregates have been observed in many aerosol samples, including those from the remote marine troposphere [*Pósfai et al.*, 1999]. There is no information, however, on the long-range transport of organic and tar ball particles. As seen in our samples, the main change that organic and soot particles experience during aging is the accumulation of ammonium sulfate on them. The smoke particles seem to provide a favorable surface for the nucleation of sulfate, and coagulation can also bring soot and sulfate together. We believe that after long-range transport biomass smoke aerosol consists primarily of internally mixed organic/sulfate and soot/sulfate particles.

[49] Apart from the C that originates from biomass burning, other sources of C (such as biogenic emissions) likely contributed to the carbonaceous material in the haze samples. All sulfate particles were coated with a carbonaceous film, even the smallest (<50 nm) particles. Sulfate probably cocondenses with organic compounds to form internally mixed, coated sulfate particles. Similar particles, with coatings of various thickness, have been observed in a variety of samples, including those from pristine marine and polluted continental environments [*Pósfai et al.*, 1999; *Pósfai and Molnár*, 2000].

[50] The results obtained from the aerosol associated with stratus clouds over the Atlantic Ocean off the coast of Namibia provide a snapshot of aerosol–cloud interactions. The results indicate that smoke particles are not necessary for the presence of persistent stratus clouds off the coast of Namibia, since the particles in, below, and above clouds were predominantly of sea-salt origin. High biological productivity, produced by strong upwelling, provides S-bearing species that convert submicrometer sea-salt particles to sulfate. In the cloud samples, a minority of the particles could have originated from biomass smoke, as indicated by their K contents (Figure 11). Whereas the cloud-nucleating particles appeared to be primarily of marine origin, the haze layers above the clouds contained aged particles from biomass smoke, creating a complicated layered system of absorbing haze and reflecting clouds.

[51] **Acknowledgments.** We thank Tom Kirchstetter and Kristy Ross for their help with sampling. This research was supported by NASA grant NAG5-9838 and Hungarian Science Foundation grant T035012. The University of Washington's participation in SAFARI 2000 was supported by NASA grants NAG5-9022, NAG5-7675, NCC5-550, and NASI-28940 and NSF grant ATM-9901624. This study is part of the SAFARI 2000 Southern African Regional Science Initiative.

References

Andreae, M. O., Soot carbon and excess fine potassium: Long-range transport of combustion-derived aerosols, *Science*, *220*, 1148–1151, 1983.

Andreae, M. O., and P. Merlet, Emission of trace gases and aerosols from biomass burning, *Global Biogeochem. Cycles*, *15*, 955–966, 2001.

Andreae, M. O., et al., Airborne studies of aerosol emissions from savanna fires in southern Africa, 2, Aerosol chemical composition, *J. Geophys. Res.*, *103*, 32,119, 1998.

Artaxo, P., E. T. Fernandes, J. V. Martins, M. A. Yamasoe, P. V. Hobbs, W. Maenhaut, K. M. Longo, and A. Castanho, Large scale aerosol source apportionment in Amazonia, *J. Geophys. Res.*, *103*, 31,837–31,847, 1998.

Buseck, P. R., and M. Pósfai, Airborne minerals and related aerosol particles: Effects on climate and the environment, *Proc. Natl. Acad. Sci. U. S. A.*, *96*, 3372–3379, 1999.

Buseck, P. R., B.-J. Huang, and L. P. Keller, Electron microscope investigation of the structures of annealed carbons, *J. Energy Fuels*, *1*, 105–110, 1987.

Cachier, H., J. Ducret, M.-P. Brémond, V. Yoboué, J.-P. Lacaux, A. Gaudichet, and J. Baudet, Biomass burning aerosols in a savanna region of the Ivory Coast, in *Global Biomass Burning*, edited by J. S. Levine, pp. 174–184, MIT Press, Cambridge, Mass., 1991.

Cachier, H., C. Liousse, P. Buat-Ménard, and A. Gaudichet, Particulate content of savanna fire emissions, *J. Atmos. Chem.*, *22*, 123–148, 1995.

Cliff, G., and G. W. Lorimer, The quantitative analysis of thin specimens, *J. Microsc.*, *102*, 203–207, 1975.

Crutzen, P. J., and M. O. Andreae, Biomass burning in the tropics: Impact on atmospheric chemistry and biogeochemical cycles, *Science*, *250*, 1669–1678, 1990.

Ebert, M., S. Weinbruch, A. Rausch, G. Gorzawski, G. Helas, P. Hoffmann, and H. Wex, The complex refractive index of aerosols during LACE 98 as derived from the analysis of individual particles, *J. Geophys. Res.*, *107*(D21), 8121, doi:10.1029/2000JD000195, 2002.

Echalar, F., P. Artaxo, J. V. Martins, M. Yamasoe, F. Gerab, W. Maenhaut, and B. Holben, Long-term monitoring of atmospheric aerosols in the Amazon Basin: Source identification and apportionment, *J. Geophys. Res.*, *103*, 31,849, 1998.

Egerton, R. F., *Electron Energy-Loss Spectroscopy in the Electron Microscope*, 410 pp., Plenum, New York, 1986.

Fuller, K. A., W. C. Malm, and S. M. Kreidenweis, Effects of mixing on extinction by carbonaceous particles, *J. Geophys. Res.*, *104*, 15,941–15,954, 1999.

Gao, S., D. A. Hegg, P. V. Hobbs, T. W. Kirchstetter, B. Magi, and M. Sadilek, Water-soluble organic components in aerosols associated with savanna fires in southern Africa: Identification, evolution and distribution, *J. Geophys. Res.*, *108*, doi:10.1029/2002JD002324, 2003.

Gaudichet, A., F. Echalar, B. Chatenet, J. P. Quisefit, G. Malingre, H. Cachier, P. Buat-Menard, P. Artaxo, and W. Maenhaut, Trace elements in tropical African savanna biomass burning aerosols, *J. Atmos. Chem.*, *22*, 19–39, 1995.

Haywood, J. M., and K. P. Shine, The effect of anthropogenic sulfate and soot aerosol on the clear sky planetary radiation budget, *Geophys. Res. Lett.*, *22*, 603–606, 1995.

Hobbs, P. V., and L. F. Radke, Cloud condensation nuclei from a simulated forest fire, *Science*, *163*, 279–280, 1969.

Hobbs, P. V., J. S. Reid, R. A. Kotchenruther, R. J. Ferek, and R. Weiss, Direct radiative forcing by smoke from biomass burning, *Science*, *275*, 1776–1778, 1997.

Hobbs, P. V., P. Sinha, R. J. Yokelson, I. T. Bertschi, D. R. Blake, S. Gao, T. W. Kirchstetter, T. Novakov, and P. Pilewskie, Evolution of gases and particles from a savanna fire in South Africa, *J. Geophys. Res.*, *108*, doi:10.1029/2002JD002352, in press, 2003.

Ikegami, M., K. Okada, Y. Zaizen, Y. Makino, J. B. Jensen, J. L. Gras, and H. Harjanto, Very high weight ratios of S/K in individual haze particles over Kalimantan during the 1997 Indonesian forest fires, *Atmos. Environ.*, *35*, 4237–4243, 2001.

Jacobson, M. Z., Strong radiative heating due to the mixing state of black carbon in atmospheric aerosols, *Nature*, *409*, 695–697, 2001.

Jury, M. R., The dry season climate of tropical southern Africa and implications for pyrogenic emissions, *S. Afr. J. Sci.*, *96*, 387–390, 2000.

Katrinak, K. A., P. Rez, and P. R. Buseck, Structural variations in individual carbonaceous particles from an urban aerosol, *Environ. Sci. Technol.*, *26*, 1967–1976, 1992.

Katrinak, K. A., P. Rez, P. R. Perkes, and P. R. Buseck, Fractal geometry of carbonaceous aggregates from an urban aerosol, *Environ. Sci. Technol.*, *27*, 539–547, 1993.

Levine, J. S., *Global Biomass Burning*, MIT Press, Cambridge, Mass., 1991.

Li, J., J. R. Anderson, and P. R. Buseck, TEM study of aerosol particles from clean and polluted marine boundary layers over the North Atlantic, *J. Geophys. Res.*, *108*, doi:10.1029/2002JD002106, 2003a.

Li, J., M. Pósfai, P. V. Hobbs, and P. R. Buseck, Individual aerosol particles from biomass burning in southern Africa, 2, Compositions and aging of inorganic particles, *J. Geophys. Res.*, *108*, doi:10.1029/2002JD002310, in press, 2003b.

Liu, X., P. Van Espen, F. Adams, J. Cafmeyer, and W. Maenhaut, Biomass burning in southern Africa: Individual particle characterization of atmospheric aerosols and savanna fire samples, *J. Atmos. Chem.*, *36*, 135–155, 2000.

Liousse, C., C. Devaux, F. Dulac, and H. Cachier, Aging of savanna biomass burning aerosols: Consequences on their optical properties, *J. Atmos. Chem.*, *22*, 1–17, 1995.

Moore, K. T., D. C. Elbert, and D. R. Veblen, Energy-filtered transmission electron microscopy (EFTEM) of intergrown pyroxenes, *Am. Mineral.*, *86*, 814–826, 2001.

Okada, K., M. Ikegami, O. Uchino, Y. Nikaidou, Y. Zaizen, Y. Tsutsumi, and Y. Makino, Extremely high proportions of soot particles in the upper troposphere over Japan, *Geophys. Res. Lett.*, *19*, 921–924, 1992.

Okada, K., M. Ikegami, Y. Zaizen, Y. Makino, J. B. Jensen, and J. L. Gras, The mixture state of individual aerosol particles in the 1997 Indonesian haze episode, *J. Aerosol Sci.*, *32*, 1269–1279, 2001.

Penner, J. E., R. E. Dickinson, and C. A. O'Neill, Effects of aerosol from biomass burning on the global radiation budget, *Science*, *256*, 1432–1433, 1992.

Pósfai, M., and Á. Molnár, Aerosol particles in the troposphere: A mineralogical introduction, *EMU Notes Mineral.*, *2*, 197–252, 2000.

Pósfai, M., J. R. Anderson, P. R. Buseck, and H. Sievering, Compositional variations of sea-salt-mode aerosol particles from the North Atlantic, *J. Geophys. Res.*, *100*, 23,063–23,074, 1995.

Pósfai, M., H. Xu, J. R. Anderson, and P. R. Buseck, Wet and dry sizes of atmospheric aerosol particles: A combined AFM-TEM study, *Geophys. Res. Lett.*, *25*, 1907–1910, 1998.

Pósfai, M., J. R. Anderson, P. R. Buseck, and H. Sievering, Soot and sulfate aerosol particles in the remote marine troposphere, *J. Geophys. Res.*, *104*, 21,685–21,693, 1999.

Reid, J. S., P. V. Hobbs, R. J. Ferek, D. R. Blake, J. V. Martins, M. R. Dunlap, and C. Liousse, Physical, chemical, and optical properties of regional hazes dominated by smoke in Brazil, *J. Geophys. Res.*, *103*, 32,059, 1998.

Reiner, T., D. Sprung, C. Jost, R. Gabriel, O. L. Mayol-Bracero, M. O. Andreae, T. L. Campos, and R. E. Shetter, Chemical characterization of pollution layers over the tropical Indian Ocean: Signatures of emissions from biomass and fossil fuel burning, *J. Geophys. Res.*, *106*, 28,497–28,511, 2001.

Roessler, D. M., F. R. Faxvog, R. Stevenson, and G. W. Smith, Optical properties and morphology of particulate carbon: Variation with air/fuel ratio, in *Particulate Carbon: Formation During Combustion*, edited by D. C. Siegla and G. W. Smith, pp. 57–84, Plenum, New York, 1981.

Sinha, P., P. V. Hobbs, R. J. Yokelson, I. T. Bertschi, D. R. Blake, I. J. Simpson, S. Gao, T. W. Kirchstetter, and T. Novakov, Emissions of trace gases and particles from savanna fires in southern Africa, *J. Geophys. Res.*, *108*, doi:10.1029/2002JD002325, in press, 2003.

Sheridan, P. J., Characterization of size segregated particles collected over Alaska and the Canadian high Arctic, AGASP-II flights 204-206, *Atmos. Environ.*, *23*, 2371–2386, 1989.

Turn, S. Q., B. M. Jenkins, J. C. Chow, L. C. Pritchett, D. Campbell, T. Cahill, and S. A. Whalen, Elemental characterization of particulate matter emitted from biomass burning: Wind tunnel derived source profiles for herbaceous and wood fuels, *J. Geophys. Res.*, *102*, 3683–3699, 1997.

Yokelson, R. J., I. T. Bertschi, T. J. Christian, P. V. Hobbs, D. E. Ward, and W.-M. Hao, Trace gas measurements in southern Africa, biomass burning smoke and haze by airborne FTIR, *J. Geophys. Res.*, submitted manuscript, 2003.

M. Pósfai and R. Simonics, Department of Earth and Environmental Sciences, University of Veszprém, POB 158, H-8200 Veszprém, Hungary. (posfaim@almos.vein.hu)

J. Li and P. R. Buseck, Departments of Chemistry/Biochemistry and Geological Sciences, Arizona State University, Tempe, AZ 85287-1404, USA.

P. V. Hobbs, Department of Atmospheric Sciences, University of Washington, Seattle, WA 98195, USA.